eDNA provides accurate population abundance estimates with bioenergetics and particle mass-balance modelling

Julien Beaulieu*[1,2], Matthew C. Yates[1,2], Dylan J. Fraser[2,3], Melania E. Cristescu[2,4] and Alison M. Derry[1,2]

[1] Département des sciences biologiques, Université du Québec à Montréal, 201 Av. du Président-Kennedy, Montréal, H2X 2J5, Montréal, QC, Canada

[2] Groupe de recherche interuniversitaire en limnologie (GRIL), Montréal, QC, Canada

[3] Department of Biology, Concordia University, 7141 Rue Sherbrooke O, Montréal, H4B 1R6, Montreal, QC, Canada

[4] Department of Biology, McGill University, 1205 Av. du Docteur-Penfield, Montréal, QC H3A 1W9, Montréal, QC, Canada

ORCID and emails:

Julien Beaulieu (corresponding author): **0000-0003-2597-8921** beaulieu.julien.2@uqam.ca
Matthew C. Yates**: 0000-0002-9199-1078** matthew.yates@outlook.com
Dylan J. Fraser**: 0000-0002-5686-7338** dylan.fraser@concordia.ca
Melania E. Cristescu: **0000-0002-0854-4040** melania.cristescu@mcgill.ca
Alison M. Derry: **0000-0001-5768-8027** derry.alison@uqam.ca

Running title:

Accurate abundance estimation from eDNA

Acknowledgements

We thank Parks Canada for logistic support, Andrew Macdonald for statistical advice, Maria Gheta for the help with the Taylor expansions, Yves Prairie for math validation, Jérôme Lemelin for the map, and Mélanie Desrochers for GIS advice. We also express our gratitude to Louis Astorg, Dylan Glaser, Brent Brooks, Shannon Clarke, Jean-Michel Matte, Justin Budyk, Mélia Lagacé, Mathilde Salamon, Sydney Urschel, and Ahmad Yaghi for field work. Research funding was provided by a Fonds de Recherche du Québec-Nature et Technologie (FRQNT) team projet grant 254557 (AMD, MEC, and DJF), a grant from the Natural Sciences and Engineering Research Council of Canada (NSERC) Strategic Project grant STPGP 494015-16 (AMD, DJF), and a NSERC Discovery Grant 2022-03706 (AMD). We thank the Groupe de recherche interuniversitaire en limnologie (GRIL) and the Faculty of Science at the Université du Québec à Montréal for providing contributions to scholarship funding for JB. MCY was supported by a FRQNT postdoctoral fellowship.

Authors contribution

JB designed the models and performed the analysis. JB and MCY contributed to the writing of the manuscript. MCY and JB collected the eDNA samples. MCY extracted the eDNA samples and conducted laboratory analyses. All authors contributed to the study design and subsequent edits to the manuscript.

Data availability statement

Data and codes will be available upon manuscript acceptance. In the meantime they can be found at: https://share.multcloud.link/share/3380ba5d-8bda-40d8-a7c7-c60298e2f1d2

Competing interests

Authors declare that they have no competing interests.

Animal care

Fieldwork was conducted under a Parks Canada Agency Research and Collection Permit (KooNP- 2017-24,999)

Abstract

Anthropogenic activities have led to an unprecedented crisis in freshwater biodiversity loss. The capacity to monitor the abundance of wild populations is critical to conserving biodiversity, but conventional physical specimen collection methods are invasive, costly, and labour-intensive. Environmental DNA (eDNA) offers a promising alternative, being easy to sample, with studies under controlled laboratory conditions showing consistent correlations between eDNA concentration and abundance. However, applying eDNA to monitor abundance remains contentious, as eDNA particle dynamics and the ecology of eDNA production can decouple this relationship in natural ecosystems. To address this, we provide a novel modeling method to produce population estimates from eDNA. We integrated bioenergetics and mass-balance frameworks to relate eDNA concentrations to freshwater fish population abundance estimated through conventional mark-recapture in Brook Trout (Salvelinus fontinalis) across nine Rocky Mountains lakes, five of which underwent size-selective harvesting over two years. Our integrated framework improved the variance explained in eDNA concentrations from 24% to 71%. The integrated model accurately distinguished most (94%) abundance estimates across populations and sampling periods, detecting both natural and harvest-induced reductions in abundance within several populations. This study is the first to empirically integrate the DNA production mechanism and particle dynamics and provide a new methodological approach enabling rapid and accurate abundance quantification. We also discuss how this new tool can be integrated in existing monitoring programs.

Key words: Environmental DNA (eDNA), Quantitative PCR (qPCR), abundance, biomass, Allometric scaling, Mass balance

Introduction

Anthropogenic activities have triggered an unparalleled biodiversity crisis in freshwater ecosystems (Albert et al., 2021). Conserving remaining biodiversity, remediating degraded ecosystems, and halting the decline of endangered populations demand rigorous monitoring and proactive aquatic ecosystem management (Ho & Goethals, 2019). However, freshwater ecosystems are notoriously difficult to monitor, with the decline in freshwater fish populations often referred to as an 'invisible collapse' (Howarth et al., 2023; Post et al., 2002). Monitoring the abundance and biomass of species in aquatic ecosystems can be particularly challenging, due to its labour- and resource-intensive nature. These challenges are magnified at larger geographic scales, where obtaining such data for remote or large freshwater waterbodies can be exceedingly difficult if not impossible. As a result, the availability of such critical data for conservation and management is often severely limited.

The analysis of environmental DNA (eDNA), which refers to DNA particles found in environmental mediums such as air, soil, and water (Ficetola et al., 2008), has revolutionised biomonitoring in natural ecosystems. The analysis of eDNA has proven highly effective for quantifying ecosystem-level biodiversity as well as detecting cryptic, rare, and traditionally difficult-to-detect species in freshwater ecosystems (Jerde, 2019; Sepulveda et al., 2020). However, numerous studies have demonstrated consistent and significant positive correlations with the concentration of eDNA and the abundance or biomass of organisms within aquatic environments; these studies have demonstrated its strong potential for providing estimates of population abundance and/or biomass in natural ecosystems (Rourke et al., 2022; Yates et al., 2019). Yet, the biological processes involved in the production of eDNA production are complex and, as a physical particle, numerous environmental parameters can impact its degradation and transportation in

natural ecosystems (Carraro et al., 2018; Stewart, 2019). Collectively, these processes can decouple the relationships between the concentration of eDNA in natural ecosystems and organism abundance/biomass (Yates, Cristescu, et al., 2021). This can be readily observed in the discrepancy between the strong correlation eDNA exhibits with abundance under controlled laboratory conditions relative to the moderate correlations observed in studies conducted within natural ecosystems (Yates et al., 2019).

Our understanding of the behaviour and dynamics of eDNA particles in natural ecosystems is constantly growing and improving through rigorous research occurring in labs across the globe. The decay rate of eDNA, for example, can depend on complex interactions among abiotic conditions (e.g., temperature, pH and UV), biotic conditions (e.g., bacterial activity), and eDNA properties (amplicon and particle size) (Brandão-Dias et al., 2023; T. Jo et al., 2019; T. Jo & Minamoto, 2021; Lamb et al., 2022; Saito & Doi, 2021a; Strickler et al., 2015). In both lentic and lotic aquatic ecosystems, eDNA particles move within water masses at different rates, which can additionally affect their deposition. The concentration measured at one place can thus be influenced by eDNA production upstream and/or its movement within currents or within thermocline layers (Jane et al., 2015; Littlefair, Rennie, et al., 2021; Pont, 2024; Shogren et al., 2017).

Metabolic and bioenergetic theory has also recently been integrated as a framework to relate eDNA production to population density and biomass by accounting for the physiological processes involved in its production (Yates et al., 2023). Metabolic processes, for example, scale allometrically with organism size (Allegier et al., 2015; Vanni & McIntyre, 2016). The strong link between eDNA production and organism metabolism implies that eDNA production likely scales allometrically within and across species (Yates et al., 2023; Yates, Wilcox, et al., 2021). Similarly, temperature has long been recognized as having a strong impact upon physiological rates within

109 poikilothermic fishes (Thornton & Lessem, 1978), which similarly extends to eDNA production
110 (Caza-Allard et al., 2022; T. Jo et al., 2019). As a result, eDNA production can be modelled as a
111 function of allometrically scaled organismal mass weighted with a temperature-dependent function
112 to adjust for the impact of the metabolic rate of the organism on eDNA production (Deslauriers et
113 al., 2017; Hanson et al., 1997; Yates, Cristescu, et al., 2021; Yates, Wilcox, et al., 2021), e.g.:

114 $$eDNA\ production = I_0 \sum_{i=1}^{N} (M_i^b) \times f(T) \quad (1)$$

115 Where I_0 is the eDNA production coefficient, N is the number of individuals in the
116 population, M_i is the mass of the ith individual, b is the allometric scaling coefficient, and $f(T)$ is
117 the temperature-dependent function, which considers the maximal metabolic rate of the organism
118 at a specific temperature (Yates, Cristescu, et al., 2021).

119 The pseudo-steady-state concentration of eDNA in natural ecosystems is a product of
120 complex dynamics between eDNA production, degradation, and transportation. Integrating across
121 these processes provides an understanding of dynamics that affect particle input and output rates;
122 as a result, the application of a mass-balance approach is ideally suited to modelling eDNA steady-
123 state concentrations, in a similar manner as classic models used for estimating phosphorus
124 concentration (Chapra & Reckhow, 1983; T. Jo et al., 2019; Sassoubre et al., 2016). If we assume
125 the concentration of eDNA to be constant in time, we can state:

126 $$eDNA_{produced} + eDNA_{imported} = eDNA_{degraded} + eDNA_{sedimented} + eDNA_{exported} \quad (2)$$

127 Where the eDNA production rate is given by the metabolic/bioenergetics function described above
128 (equation 1), and eDNA imported describes the rate eDNA enters the system from up-stream
129 sources. The rate at which eDNA is degraded is typically described by an exponential decay curve

130 as a function of temperature, pH, and other factors that can influence eDNA degradation rate, with
131 'k' being the degradation constant (Kagzi et al., 2022). No research has yet examined eDNA
132 sedimentation rates independent of particle decay, but sedimentation of particles in the water are
133 also typically modeled using exponential decay curves (Chapra & Reckhow, 1983). The rate at
134 which eDNA is exported (i.e., transported) refers to the amount of eDNA exiting by the outflow of
135 a water body, which can be calculated as the outflow times the concentration at the surface (Chapra
136 & Reckhow, 1983). By developing equation 2 and isolating eDNA concentration, the formula can
137 be expressed as:

138 $$[eDNA]_{water} = \frac{W}{Q + (k_{deg} + k_{sed})V} \quad (3)$$

139 Where $[eDNA]_{water}$ is the eDNA concentration in the water, W is the average eDNA production
140 (equation 1) plus the average eDNA importation from upstream, V is the volume of the water body,
141 Q is the water flow rate, K_{deg} is the degradation constant at these specific environmental conditions,
142 and K_{sed} is the sedimentation rate.

143 Modelling that integrates both bioenergetics and mass balance approaches to eDNA
144 concentrations to estimate total population abundance and biomass in natural ecosystems remains
145 unexplored. Yet, it holds considerable potential for improving the capacity to link eDNA
146 concentrations observed in natural ecosystems to wild population abundance. With refined
147 quantitative knowledge on eDNA production, decay, and transport rates, eDNA could become a
148 cost-effective tool for species quantification in aquatic systems (Huang et al., 2022; Yates,
149 Cristescu, et al., 2021). To date, however, no study has integrated across all these processes to
150 generate total population abundance/biomass estimates in natural ecosystems.

151 We investigated the application of an integrated bioenergetics and mass-balance approach
152 to estimate population abundance from eDNA concentrations observed in natural lentic aquatic
153 ecosystems. Our aims were to: i) differentiate total abundance *across* populations; and ii) detect
154 changes in total abundance *within* populations. To accomplish these objectives, we quantified
155 Brook Trout (*Salvelinus fontinalis*) eDNA concentrations and total abundance (using mark-
156 recapture techniques) in nine Rocky Mountain lakes (CA) across two seasons for two years. This
157 was done while simultaneously conducting an annual experimental size-selective harvest in five of
158 the nine lakes to manipulate total abundance and population density across the study period. We
159 then investigated the added power of an integrated bioenergetics and mass-balance approach in
160 explaining observed eDNA concentrations compared to approaches previously taken in the
161 literature. This included: i) correlating eDNA concentrations as a linear function of population
162 abundance, and ii) correlating eDNA concentrations as a function of allometrically scaled
163 population biomass. We predicted that taking an integrated bioenergetic and mass-balance
164 approach that holistically accounts for the processes involved in eDNA production, degradation,
165 and transportation would increase the power of eDNA to detect changes in the abundance and
166 biomass of Brook Trout across space and time.

167

168 **Methods**

169 ***Study system***

170 Our study included nine headwater mountain lakes in the Canadian Rockies, located within
171 Banff, Yoho, and Kootenay National Parks (Canada; Fig. 1). The nine study lakes contain fish
172 communities largely dominated by Brook Trout (*Salvelinus fontinalis*) that were introduced to the
173 lakes between the 1920s and the 1970s and are now invasive in the region (Messner et al., 2013).

174 Six of the lakes were solely inhabited by Brook Trout, while the three other had fish communities
175 also containing one to five other species. Five of the nine study lakes were subjected to a size-
176 selective harvest treatment where approximately 64 % of each population was removed each year
177 during Fall from 2017 to 2019, targeting the largest-bodied individuals for harvest. At the
178 beginning of the experiment (2017), the Brook Trout populations differed in density and population
179 size structure between lakes, and the harvesting treatment was successful at inducing changes in
180 population demography over the duration of the three-year experimental manipulation (Matte et
181 al., 2023). The other four study lakes were monitored as references in which Brook Trout
182 populations were not directly manipulated (Appendix 1). All lakes are small, cold, oligotrophic
183 headwater lakes, but they span a 1000 m elevation gradient over which there are differences
184 between lakes in temperature, pH, and nutrient concentrations (Appendix 1; Trépanier-Leroux et
185 al., 2023).
186
187 ***Field sampling of eDNA***
188 Environmental DNA samples were collected each year between 2018 and 2019 for two time
189 periods: i) in Summer before harvesting (June/July); and ii) in the Fall (September) following
190 harvest activities. A systematic stratified survey design was used to collect eDNA samples, in
191 which 4 samples each were collected from the pelagic and littoral zones of each study lake. In the
192 littoral zones, eDNA sample sites were distributed equidistantly around the perimeter of the lake.
193 Littoral samples were collected approximatively 1-3 m from the shore at a minimum depth of 30
194 cm from the surface, but approximately 15 cm above the lake bottom. In the pelagic zones, four
195 samples were collected at equidistant intervals across a transect that followed the longest axis of
196 the lake and went through the lake center (defined as the midpoint of the longest axis). Pelagic

197 samples were collected at a depth of 0.5 to 1 m from the surface. Water samples were collected
198 with 700 ml Whirl-Pak™ bags from a canoe assigned to sample a single specific lake, or from an
199 inflatable kayak, which was decontaminated 48 hours prior with a 2% regular strength household
200 bleach solution for 15 min (including paddle and lifejacket) and left to dry in the sun.

201 Water samples were immediately filtered on the lakeshore on a water filtering manifold
202 (Wildco, Florida, USA) that was decontaminated with a 20-30% bleach solution 2-12 h prior to
203 sampling. Manifold components were stored individually in plastic zippered bags after bleaching
204 and during transportation. All samples were stored in the shade prior to sampling, and all filtering
205 was conducted in the shade under a tarp. One litre of water from each of the eight water sampling
206 sites per lake was filtered through a 0.7 µm glass fibre filter (GE Healthcare Life Sciences, Ontario,
207 Canada) using a vacuum hand pump (Soil Moisture, California, USA). Vacuum pumps were
208 decontaminated between lakes by wiping with a 30% bleach solution and resting for 10 minutes,
209 after which they were wiped with distilled water to remove residual bleach. All littoral samples
210 were filtered on one manifold, and all pelagic samples were filtered on another to prevent cross-
211 contamination between samples from different lake zones. As a negative control, 500 mL of
212 distilled water was filtered prior to filtering lake samples. After filtration, filters were folded using
213 metal forceps (decontaminated using a 30% bleach solution for 15 minutes) and stored in a sterile
214 2 mL microcentrifuge tube containing 700 µL of ATL buffer that was then individually placed in
215 a plastic zippered bag and stored in a cooler bag that was decontaminated by wiping with a 30%
216 bleach solution. If a filter became clogged (i.e. < 1 L of water was filtered), the final volume of
217 water filtered was recorded and the sample was then stored in buffer. Samples were then
218 transported in a cooler bag with bleached frozen gel packs to Kootenay Crossing (BC, Canada),
219 where they were placed in a second zippered plastic bag and stored in a -20 °C freezer. At the end
220 of the sampling season, all samples were transported to Montreal on dry ice and placed in a -80 °C

221 freezer until extraction. All protocols for contamination prevention in the field, as well as during
222 transport and storage can be found in Appendix 2.

223

224 ***Laboratory analysis of eDNA***

225 DNA was extracted from each filter using Qiagen DNeasy Blood and Tissue™ kit and
226 Qiashredder™ columns following a modified extraction protocol (see Yates et al. (2021a) for more
227 details). Extracted DNA was eluted into 130 µL of AE buffer and stored in a clean -20 °C freezer
228 solely dedicated to the storage of extracted eDNA product (i.e. no post-PCR products or tissue
229 samples). An extraction blank of 700 µL of ATL buffer was included in all batches as a control.
230 Methods for contamination prevention are detailed in Supplementary Information (Appendix 2).

231 Brook Trout eDNA concentration was quantified using quantitative PCR (qPCR) with the
232 *cyt b* TaqMan minor groove assay (BRK2) described in (Wilcox et al., 2013). For details on PCR
233 reaction preparation, component concentrations, standard curve preparation, and cycling
234 conditions, see (Yates, Glaser, et al., 2021). All samples were run in triplicate in a 20 µL reaction
235 volume with 5 µL of template DNA on a Stratagene MX 3000P thermal cycler. Reactions were
236 spiked with an internal positive control (IPC) to test for inhibition, which was defined as a 1 > Ct
237 shift in the IPC relative to a reaction containing 5 µL of nuclease-free ultrapure water. If inhibition
238 was detected, samples were diluted down to 3 µL and re-run. Brook Trout eDNA concentrations at
239 each site were calculated by averaging replicate values, and final copy number data were converted
240 to eDNA concentration per L of water filtered (copies/L). Standard curve R^2 values for the qPCR
241 plates ranged from 0.98-0.99, and reaction efficiency varied between 83.1 and 98.6%. The
242 efficiency of two of the 11 plates was suboptimal (< 85%). However, data generated from these
243 two plates were retained, as their inclusion did not impact results (Appendix 3). Samples associated

with negative controls that contained more than 5 copies/rx (on average) were removed from the analysis due to contamination concerns (Cobb Lake samples from Fall 2019). Most samples collected across lakes per sampling period (26/36 sampling events) showed no contamination, while the remaining contamination in field controls was low enough to not impact the estimated lake eDNA concentrations.

Brook Trout mark-recapture and population size structure estimation

Mark-recapture studies of Brook Trout were conducted in all lakes during May and June in both 2018 and 2019 (Matte et al., 2023; Yates, Glaser, et al., 2021). The exception was Cobb Lake where, in addition to mark-recapture sampling in May/June, a series of isolated marking events continued until September for both years. Fish were captured using a combination of fyke nets, angling, and backpack electrofishing. Large (1 m hoop diameter, 2 cm mesh) and small (0.7 m hoop diameter and 0.8 cm mesh) fyke nets were distributed around the perimeter of lakes with the lead attached to shore and the end of the trap facing the center of the lake. Nets were checked daily. Angling was used to supplement Brook Trout capture efforts at sites where fyke catchability was low (predominantly Cobb Lake). Marks were also assigned to Brook Trout captured by electrofishing the shore and inlets/outlets of lakes.

Captured Brook Trout were anesthetized using clove oil and measured for fork length (± 1 mm) and mass (± 0.1 g). Any unmarked Brook Trout were gastrically tagged with a BioMark HPT8 pre-loaded Passive Integrated Transponder (PIT) tag (Boise, Idaho, USA). Only Brook Trout greater than or equal to 80 mm were tagged to reduce tagging mortality. Other species, when present, were not tagged. The tag number of any recaptured Brook Trout was recorded. Recovered fish were released in the center of the lake to standardize release location and promote mixing. Marking ceased once recapture ratios approached twenty five percent for several consecutive days

267 to standardize marking efforts across all populations and to ensure that enough Brook Trout were
268 tagged to facilitate estimation of census size (Nc) with credible intervals within 10% to 25% of
269 true values, following general methodologies reviewed in (Krebs, 2009; Matte et al., 2023).

270 To obtain representative snapshots of the size structure of each Brook Trout population
271 before and following harvest, population size structure estimates were conducted in August 2018
272 and 2019 (Matte et al., 2023). The exception was Cobb Lake where size structure assessments
273 continued to October 12th. During mark-recapture, fyke-nets were deployed in littoral zone areas
274 extending to the centre of the lake and, as a result, size-structure assessments obtained from fyke
275 nets may be more biased towards small-medium bodied individuals that tend to prefer littoral
276 habitats (Tiberti et al., 2017). To obtain a relatively unbiased estimate of population size structure,
277 Brook Trout were captured in large and small sinking mixed mesh gillnets with clear monofilament
278 distributed throughout the lake. Large mixed-mesh gillnets were 15.6 m long, 1.8 m deep and had
279 an equal area of 64-51-89-38-76 mm mesh panels. Small mixed-mesh gillnets were 12.5 meters
280 long, 1.8 meters deep, and consisted of an equal area of 32-19-38-13-25 mm mesh panels. Such
281 index nets are widely used in North America for size structure assessments (Bonar et al., 2009;
282 Hubert et al., 2012; Johnson, 1983; Post et al., 1999; Ward et al., 2012), as these capture a
283 representative size/age structure of fish populations (Morgan, 2002). Nets were checked daily and
284 moved to different locations across the lake, to capture a representative sample of Brook Trout in
285 each lake. Sampling ceased when approximately five to ten percent of the population was captured,
286 apart from Cobb Lake where the harvested fish were also included for size structure assessment
287 such that approximately 71% of individuals were used. Captured Brook Trout were euthanized
288 with clove oil, PIT tags were recorded, and length/mass data were collected as described for the
289 marking period.

290 Schnabel population abundance estimates were used to estimate the abundance of Brook
291 Trout in a lake (Matte et al., 2023; Schnabel, 1938). All size structure assessment removals were
292 pooled together into one final sampling event for the population abundances which controlled for
293 the removal of marks at large. Note that abundances only account for Brook Trout greater than the
294 minimum tagging size (80 mm fork length), which correspond to all individuals age 1 and older
295 (Matte et al., 2023). All population abundace estimates were conducted in R (CoreTeam, 2020)
296 with the mrClosed function from the Fisheries Stock Assessment package FSA (Ogle, 2015).
297 Credible intervals for Schnabel population abundance estimates followed recommendations from
298 (Seber, 2002) as implemented in the FSA package.

299 ***Size-selective harvesting of Brook Trout***

300 Populations at Cobb, Mud, Olive, Ross, and Temple lakes were harvested annually with
301 size-selective gillnets (25– 89 mm mesh) targeting the top 75% (but effectively harvesting the top
302 64% on average) of individual body sizes according to the size distributions estimated during stock
303 assessment (i.e. depleting the largest size classes sequentially until the only remaining individuals
304 were in the lowest 25% quartile of the original size structure). Details can be found in Matte et al.
305 (2023).

306 ***Lake temperature and its effect on the physiology of eDNA production***

307 To adjust for maximal metabolic rate of fish at a given temperature, we used a temperature-
308 dependent function specific to Brook Trout published from previous empirical studies (Deslauriers
309 et al., 2017; Hartman & Cox, 2008). Temperature data were constituted of both high frequency (15
310 min) surface temperature from data loggers (Onset Hobo®; UA-002-64, Onset Computer
311 Corporation, Cape Cod, Massachusetts) and vertical profiles from a YSI multiparameter sonde
312 (model 10,102,030; YSI Inc.). The dataloggers were deployed at 0.5 m from the surface in June

313 and retrieved in September. The YSI vertical profiles were taken at the deepest point of the lake at
314 the same time as eDNA sampling, except six lakes in Fall 2019 where a YSI sonde malfunction
315 necessitated us to use data from the same time period in 2018 as a proxy. There was an
316 approximately +/- 2°C difference between Fall 2018 and 2019 for the lakes that had YSI data for
317 both seasons and as a result, this likely had a negligible impact on model estimates. When possible,
318 mean surface temperature over the interval from two weeks before to two weeks after each eDNA
319 sampling event per lake was used as input in the temperature-dependent function in the eDNA mass
320 balance model. However, due to logistic constraints and material failures, some lakes and sampling
321 periods had temperature data for only a subset of the time intervals or only the epilimnion mean
322 temperature from the YSI vertical profiles. A table with the lakes, dates, and temperature data can
323 be found in the supplementary materials (Appendix 4).

324 ***Lake hydrology***

325 To calculate the rate of lake outflow, lake watershed area was estimated using the flow
326 direction and flow accumulation hydrologic models from ArcGIS pro V.3.2. The input data were
327 15 m resolution Digital Elevation Models (DEM) for 7 out of the 9 study lakes. However, the 15
328 m resolution was too low to effectively determine the watershed for two of the lakes (Mud and
329 McNair). Fifteen m resolution DEM are publicly available form the Government of Canada and
330 under Open Government Licence (https://open.canada.ca/en/open-government-licence-canada).
331 The Mud and McNair lakes required high resolution data, but none were available for their area.
332 The Mud Lake watershed area was therefore estimated by process of elimination by estimating the
333 watershed area of the surrounding larger water courses. The remaining area that was not part of
334 any other watershed was assumed to be Mud Lake's watershed. We could not obtain watershed
335 area for McNair Lake. This missing data was handled with data imputation before fitting using the

336 mice package (Buuren & Groothuis-Oudshoorn, 2011). The lake outflow rate was estimated by
337 multiplying each lake watershed area with the flux per area of watershed from hydrological stations
338 from the same area (Kootenay: Kootenay River: 50.886944, -116.045833; Banff: Pipestone River:
339 51.433056, -116.174722; Environment and Natural Resources Canada, 2024). The rate of outflow
340 for each lake at each sampling period was calculated as the mean outflow from two weeks before
341 the sampling date to two weeks after.

342 ***Lake volume and epilimnion volume***

343 Detailed bathymetric maps and lake volume produced by high frequency sonar were
344 available for only four study lakes (Temple, Olive, Helen, and Margaret). For the remaining five
345 study lakes, we used older bathymetric maps from Parks Canada that were georeferenced and
346 digitised in ArcGIS Pro. The depth between isobaths were interpolated using Bayesian Kriging
347 method. The epilimnion volume was taken as the input in the mass balance model (equation 5 and
348 8). Epilimnetic volume was chosen because eDNA samples were collected from the epilimnion of
349 each lake; this was done because most study lakes undergo thermal stratification during Summer,
350 and because Brook Trout spend most of their time feeding and resting in surface waters (Tiberti et
351 al., 2017). Additionally, research has demonstrated that the transfer of eDNA across the
352 thermocline is limited during lake stratification (Littlefair, Hrenchuk, et al., 2021). The epilimnion
353 volume was calculated as the mean thermocline depth times the lake surface area from the
354 bathymetric maps. The mean thermocline depth was calculated from two YSI sonde vertical
355 temperature profiles per Summer. For the study lakes that were not thermally stratified (assessed
356 from the YSI vertical temperature profile) at the time of eDNA sampling period, total lake volume
357 (estimated from the bathymetric maps) was used as input in mass-balance models for that time
358 point because eDNA signal is expected to become homogenous throughout the water column

during mixing (Littlefair, Hrenchuk, et al., 2021). The extent of thermal stratification during the Fall 2019 could not be quantified due to the malfunction of the YSI sonde. Lakes that were mixed in Fall 2018 were therefore also assumed to be mixing in Fall 2019 except for Margaret Lake, where stratification was very weak in Fall 2018 and it was not fully mixed. As Fall 2019 was colder than Fall 2018, we assumed that Margaret Lake was mixing in Fall 2019; this increased model fit for this lake.

Statistical analyses

Constructing and evaluating an integrated bioenergetics/mass-balance model

To obtain a representative mean eDNA concentration for each lake and sampling period, the littoral and pelagic samples were weighted according to the littoral and pelagic zone area in each lake. The littoral zone was defined as the area where the depth is bellow or equal to 2 m. To parameterise the mass balance model (equation 3), a non-linear Bayesian model with informative priors was used. The parameters estimated were I_0 (eDNA generation coefficient), b (allometric scaling coefficient), and k (a combined degradation and sedimentation constant). Although equation 3 has both the degradation constant k_{deg} and the sedimentation constant k_{sed}, the current state of knowledge on eDNA degradation and sedimentation does not allow for a precise estimate of the values for k_{deg} and k_{sed}, and so one "disappearance constant" k was parameterised in the model as the sum of both (equation 4).

$$[eDNA]_{Lake} \sim \frac{I_0 \sum_{i=1}^{N} (M_i^b) \times f(T)}{Q + kV} \quad (4)$$

The model was fitted with a Gaussian distribution, four chains, 10 000 iterations, and *adapt_delta = 0.99*. A lake specific and temperature dependant k parameter was estimated to account for potential differences in degradation rates between lakes and in time, and a sampling period specific

eDNA generation coefficient (I_0) to account for season and sampling period effect on mean Brook Trout eDNA concentrations observed across lakes (Gaudet-Boulay et al., 2023), either due to ecological differences in the eDNA production coefficient (I_0) across seasons or potential (unintentional) methodological differences in sampling. For all analysis, $\sum_{i=1}^{N}(M_i^b)$ was approximated using the Taylor expansion for the first moment (Beaulieu et al., 2024) such that equation 4 becomes:

$$[eDNA]_{Lake} \sim \frac{I_0 f(T) \times N(\bar{M} + \frac{\sigma_M^2}{2} b(b-1)\bar{M}^{b-2})}{Q + kV} \quad (5)$$

Where $\bar{M}$ is the mean mass of the fish and σ_M^2 is the variance of the mass of the fish. The priors used were:

$$\begin{gathered}
\ln(I_0) \sim normal(10, 2) \\
b \sim beta(2.8, 1.2) \\
\ln(k) \sim normal(-0.7, 0.1) \sim \beta \times Temperature + (1 \mid Lake) \\
Standard\ deviation_{K\ lake} \sim exponential(3) \\
\beta \sim normal(0.1, 0.05) \\
\sigma \sim \theta + N^{\alpha} \\
\alpha \sim normal(0,0.5),\ lb = 0 \\
\theta \sim normal(0,1),\ lb = 0
\end{gathered}$$

The prior on I_0 ensured posterior predictions were the correct order of magnitude, the prior on b ensured values were between 0 and 1 with a higher probability density around 0.7, which is approximately the b value estimated from Brook Trout bioenergetic models and expected based on bioenergetic theory (Deslauriers et al., 2017). The prior for k ensured values corresponding roughly to the expected values based on Lamb et al. (2022). eDNA data were scaled to Kilocopies m^{-3} to avoid working with very large numbers. The prior on sigma accounted for heteroscedasticity and increases variance with total abundance (N), and α and θ have a lower bound (lb) at zero.

Comparing the mass balance eDNA approach to other existing models

Most previous studies examining relationships between eDNA concentrations and organism abundance/biomass typically directly regress observed eDNA concentrations against estimates of abundance and/or biomass (Yates, Glaser, et al., 2021). To evaluate the relative importance of accounting for both bioenergetics and particle dynamics (i.e., mass balance modelling), we also fitted models in which eDNA concentrations were directly related to both population biomass (equation 6) and allometrically scaled biomass (equation 7 and Yates, Cristescu, et al., 2021; Yates, Glaser, et al., 2021). Both models were fitted assuming a Gaussian distribution:

$$[eDNA]_{Lake} \sim intercept + \beta \frac{N \times \bar{M}}{lake\ area\ (ha)} \tag{6}$$

$$[eDNA]_{Lake} \sim \frac{I_0 \sum_{i=1}^{N} (M_i^b)}{lake\ area\ (ha)} \approx \frac{I_0 \times N(\bar{M} + \frac{\sigma_M^2}{2}\, b(b-1)\bar{M}^{b-2})}{lake\ area\ (ha)} \tag{7}$$

With the priors:

$$\begin{gathered} \ln(I_0) \sim normal(0, 5) \\ b \sim beta(2.8, 1.2) \\ \sigma \sim cauchy(0, 5) \end{gathered}$$

The performance of the different models was compared using the Bayes R^2, looIC, and the value of the slope comparing the predicted and measured eDNA concentrations (the closer to one the better).

Evaluating the efficacy of eDNA to estimate population abundance

We used our integrated bioenergetics/mass-balance approach to derive estimates of population abundance to compare their precision and accuracy relative to estimates of abundance derived from mark-recapture. Specifically, we were interested in evaluating the efficacy of eDNA

to both i) differentiate total abundance *across* study populations; and ii) detect changes in total abundance *within* a population over time (i.e., population reductions due to harvesting). To produce posterior estimates of total abundance for each of the populations during each sampling period using the mass balance approach, *N* was isolated from equation 5 and the model was refitted with the same priors. Additionally, season and sampling period can have a strong effect on mean Brook Trout eDNA concentrations observed across lakes (Gaudet-Boulay et al., 2023), either due to ecological differences in the eDNA production coefficient (I_0) across seasons or potential (unintentional) methodological differences in sampling. A sampling-period specific I_0 was therefore also fitted in the model. Equation 5 then becomes:

$$N \sim \frac{[eDNA]_{Lake} \times (Q + kV)}{I_0 f(T) \times \left(\bar{M} + \frac{\sigma_M^2}{2} b(b-1)\bar{M}^{b-2}\right)} \tag{8}$$

With the priors:

$$\begin{gathered}
\ln(I_0) \sim normal(10, 2) \\
b \sim beta(2.8, 1.2) \\
\ln(k) \sim normal(-0.7, 0.1) \sim \beta \times Temperature + (1 \mid Lake) \\
Standard\ deviation_{K\ lake} \sim exponential(3) \\
\beta \sim normal(0.1, 0.05) \\
Standard\ deviation_{\log(I_0\ Sampling\ period)} \sim exponential(3) \\
\sigma \sim \theta + N^{\alpha} \\
\alpha \sim normal(0,0.5),\ lb = 0 \\
\theta \sim normal(0,1),\ lb = 0
\end{gathered}$$

In this model, we also accounted for the measurement error on the mark-recapture total abundance estimates (McElreath, 2018). We also examined the efficacy of the integrated eDNA model to differentiate population biomass, which can be estimated from the integrated eDNA model (equation 8) for each population by multiplying the posterior distribution of *N* values by the mean mass of each population. Note that these models do not test the relationship between eDNA

concentration and numerical abundance, but instead our ability to estimate numerical abundance from the markers' concentration when considering a known mass distribution. The performance of the model was assessed using Bayesian R^2 and the number of abundance estimates from eDNA that overlapped with mark-recapture (and their respective 95% credible intervals).

Examining potential sources of bias

To assess the presence of systematic bias of the model, a Bayesian mixed model with non-informative priors was fitted with the z-score of each eDNA prediction as the independent variable. The fixed effects were mark-recapture abundance estimates, elevation, lake thermal mixing status (yes = stratified or no = mixed), season (Summer or Fall), lake area and experimental treatment (harvested or reference lake). We included interactions between thermal mixing status and elevation, between season and treatment, and between season and elevation. Lake was included as a random intercept to account for non-independence. This bias testing model was performed on the outputs of the eDNA mass-balance models, including sampling period specific I_0.

Can the nine lakes calibrate a model to predict abundance in novel systems?

Due to repeated sampling within and across years, the model described in equation 8 can estimate lake-specific degradation constants and sampling period specific I_0, and is thus well-suited to monitoring abundance within and across this specific set of nine study lakes. However, this model cannot be extended to estimate population abundance in a lake without pre-existing data (e.g., where a lake specific k is unknown). To explore the efficacy of this approach to estimate abundance in lakes (equation 8) without pre-existing baseline data, we fitted two additional models: i) a model with lake specific k but no sampling period specific I_0 to assess the importance of accounting for local, lake-specific eDNA degradation rates (referred to as equation 8.1 in the results) and ii) a model without a lake specific eDNA disappearance constant (k) nor sampling

457 period specific I_0 to assess how a generalizable model would perform as well as the importance of
458 a sampling period specific eDNA generation coefficient (referred to as equation 8.2 in results). The
459 performances of these different models were compared using Bayesian R^2 values. All analyses
460 were performed in *R* (CoreTeam, 2020) using the *brms* package (version 2.18.0) (Bürkner, 2018).

461

462 **Results**

463 Brook Trout abundance varied significantly between lakes with estimates ranging from 72
464 (46 – 117) to 3173 (2644 – 3965) individuals based on mark-recapture. Temporal variation in
465 population abundance was particularly pronounced in the size-selectively harvested lakes, where
466 annual harvest ranged from 46.8% to 92.7% of the population. Despite these high harvest levels,
467 compensatory effects allowed populations to partially recover between harvesting treatments
468 (Matte et al., 2023). Natural mortality also contributed to population changes. For instance, in Dog
469 Lake, population abundance declined by 32% between the Summers of 2018 and 2019, reflecting
470 substantial non-harvest losses.

471 *Comparing the mass balance eDNA approach to other existing models*

472 The eDNA mass balance model explained more variability in eDNA concentration and was
473 more accurate than a linear regression with biomass or allometrically scaled biomass (Table 1, Fig.
474 2). While all three models had little bias, biomass alone explained only 24% of the variation in
475 predicted eDNA values (Bayes R^2). This increased to 44% after integrating the effect of allometry
476 on eDNA production (e.g., allometrically scaled mass). Integrating both bioenergetics and mass-
477 balance modelling approaches substantially improved upon this, with the integrated model
478 explaining 71% of the variation in observed eDNA concentrations.

479 *Evaluating the efficacy of eDNA to estimate population abundance*

480 Total abundance estimates derived from eDNA concentration data (equation 8) effectively
481 differentiated populations across spatial and temporal scales (Fig. 3). The study populations
482 exhibited a substantial gradient in total abundance across lakes, with the smallest population
483 exhibiting a 32-fold difference in abundance relative to the largest population. At this scale, the
484 integrated eDNA model was very effective at differentiating abundance across populations (Fig 3).

485 Variations in abundance were significantly greater among populations than within
486 populations, even for populations that exhibited substantial within-population declines due to size
487 selective harvesting manipulations. Within a population, abundance levels were more consistent
488 across seasons and years (Fig. 3 and Fig. 4). Yet, even within populations, the accuracy and
489 precision of the integrated eDNA model was sufficient to detect changes across seasons and years
490 in several of the harvested lakes (e.g., Olive and Temple), as well as natural fluctuations in
491 abundance across control populations (e.g., Margaret and Dog lakes).

492 The majority (32/35 or 94%) of the total abundance estimates derived from the eDNA mass
493 balance model (equation 8) fell within the 95% credible intervals for total abundance estimated by
494 mark-recapture (Fig. 3 and 4). The integrated eDNA model similarly proved effective at
495 differentiating population biomass across space and time, also overlapping with mark-recapture
496 estimates in 32/35 of the cases. The biomass estimates from the integrated eDNA model were
497 highly correlated with estimates derived from mark-recapture (Bayes $R^2 = 0.89$) (Fig. 5) and, as
498 with abundance, enabled the clear differentiation of biomass both across and within populations
499 (Fig. SM1).

500 *Examining potential sources of bias*

When testing for different biases of the eDNA total abundance estimates, there was no significant systematic bias detected related to the total Brook Trout abundance nor lake size. There was a non-significant tendency to generate larger abundance estimates in lakes experiencing experimental harvesting during the Fall seasons (e.g., Ross and Mud at Fall 2019) compared to mark-recapture (Fig 4, Table 2, and Appendix 5).

Can the nine lakes calibrate a model to predict abundance in novel systems?

Incorporating a lake specific eDNA disappearance constant (*k*; the sum of the sedimentation and degradation constant) significantly improved model performance, as demonstrated by the large standard deviation on a general *k* estimated across lakes and the reduction in model performance when removing lake specific *k* (equation 8.2), with the Bayes R^2 dropping from 0.75 to 0.51 (Table 1 and Appendix 6). The effect of accounting for a sampling period specific eDNA generation coefficient (I_0; equation 8.1) had no effect on model performance. Brook Trout abundances predicted from the eDNA mass balance model that lacked a sampling period specific I_0 (equation 8.1) also fell within the 95% credible intervals for total abundance estimated by mark-recapture for 31/35 estimates (Appendix 5).

Discussion

There is an increasing demand for abundance data to understand and manage ecosystems (Huang et al., 2022). Yet, the application of eDNA to aid in quantifying the abundance or biomass of aquatic organisms remains a controversial topic (Parsley et al., 2024; Rourke et al., 2022; Yates et al., 2019). This stems from the complex interplay of biotic and abiotic factors that influence eDNA production, degradation, and transportation in natural aquatic environments (Yates,

522 Cristescu, et al., 2021). These are considerably more variable across space and time in natural
523 ecosystems relative to controlled laboratory settings (Yates et al., 2019).

524 Herein, we demonstrate that eDNA can provide estimates of organism abundance and
525 biomass comparable in precision and accuracy to mark-recapture. However, achieving this
526 accuracy required accounting for biotic and abiotic factors that affect its distribution in natural
527 ecosystems, namely the ecology of its production and the dynamics of the physical eDNA particles.
528 Applying our integrated bioenergetics and mass balance approach to model quantitative eDNA
529 signals greatly improved the relationship between eDNA concentration and total abundance
530 estimates in the study ecosystems, compared to a basic linear correlation between either eDNA and
531 biomass or eDNA and allometrically scaled biomass. Our integrated approach allowed for the
532 accurate differentiation of population abundance and biomass across study populations (i.e., space)
533 based on lake eDNA concentrations. Quantifying the concentration of eDNA within the study lakes
534 also facilitated the prediction or monitoring of temporal changes in fish abundance/biomass over
535 time within several populations.

536 Previous research has demonstrated the influence of several factors on eDNA concentration
537 and dynamics, including transportation (Carraro et al., 2018; Sepulveda et al., 2020; Shogren et al.,
538 2017), degradation (Carraro et al., 2018; T. Jo et al., 2019; T. Jo & Minamoto, 2021; Strickler et
539 al., 2015), temperature (Caza-Allard et al., 2022; T. S. Jo, 2023), and fish metabolic rate (Yates,
540 Cristescu, et al., 2021; Yates et al., 2023; Yates, Wilcox, et al., 2021). However, our study is the
541 first to integrate mass balance processes with bioenergetics to relate eDNA concentration to total
542 population abundance in natural ecosystems. We empirically demonstrate that eDNA could
543 represent a time- and cost-effective tool for generating total abundance estimates, with sufficient

544 precision to detect changes in abundance, by integrating relatively simple-to-collect environmental
545 and ecological data.

546 ***Evaluating the efficacy of eDNA to estimate population abundance***

547 eDNA abundance estimates corresponded to mark-recapture abundance estimates in 32 out
548 of 35 cases (91%) when considering the 95% credible interval. All three discrepancies were likely
549 due to issues associated with our unique study design causing the violation of assumptions in our
550 mass-balance modelling (i.e. experimental harvesting), and/or the violation of assumptions
551 associated with the mark-recapture estimates for populations in the Fall sampling periods (e.g., no
552 natural mortality or emigration).

553 There was a non-significant trend wherein estimates of abundance derived from eDNA
554 tended to be higher than for mark-recapture in harvested lakes in the Fall. The time necessary for
555 eDNA concentrations to stabilize depends on eDNA degradation rate, which can be impacted by
556 amplicon size, temperature, and potentially UV radiation, pH, and microbial activity (Lamb et al.,
557 2022). The values estimated by the eDNA mass balance model for the *k* degradation parameter (the
558 eDNA "disappearance rate", or the sum of the sedimentation and degradation rates) corresponded
559 to expectations based on previous controlled experiments. Notably, meta-analysis reported
560 degradation constant values between 0–0.4 h^{-1} or 0 – 9.6 day^{-1} in freshwater ecosystems (T. Jo &
561 Minamoto, 2021; Lamb et al., 2022). We obtained an average *k* value estimate ranging from 1.3 to
562 6.9 day^{-1} depending on lakes and water temperature, with a mean of 3.06 day^{-1}. Based on the eDNA
563 disappearance constant *k* estimated by the model, the outflow rate, and the Summer eDNA
564 concentration in each lake and each year, we estimated that one to fifteen days would be necessary
565 for eDNA turnover in this study system (Appendix 8). For logistical reasons (i.e., the harvesting
566 treatment took a substantial amount of time and extended late in the season), there were generally

567 fewer than seven days between the end of harvesting and eDNA sampling within several of the
568 harvested lakes, which is less than the turnover rate in most cases. This was especially the case for
569 Mud and Ross lakes in Fall 2019, which represent two of the three significant discrepancies
570 between eDNA and mark-recapture. A tendency for the integrated eDNA model to overestimate
571 fish abundance following harvesting could be explained by many eDNA copies being released
572 during harvesting. Carcasses can be a significant source of eDNA (Dunker et al., 2016) and often
573 remained in nets for 24 - 48h, thus increasing the initial amount of eDNA and time before
574 stabilisation back to a steady state concentration.

575 There was also one case where the eDNA estimate weas lower than mark-recapture
576 estimates in Dog Lake in Fall 2019. An instinctive response may be to attribute this discrepancy to
577 error in the integrated eDNA model. However, this discrepancy between the eDNA-derived and
578 mark-recapture abundance estimates could be attributable to violations of the assumptions of the
579 mark-recapture methodology employed. Mark-recapture estimates demonstrated that Dog Lake
580 exhibited a substantial natural decline in abundance between 2018 and 2019. While mortality was
581 assumed to be negligible between Summer and Fall, we do not actually know when this mortality
582 event occurred because mark-recapture studies occurred in the spring and Summer of each year.
583 Results from the eDNA model could imply that the natural mortality event may have occurred
584 during both Summer 2018 and 2019. In these cases, eDNA may more accurately reflect the
585 abundance of fish in the study lakes than mark recapture estimates, for which we assumed there
586 was no natural mortality nor emigration for the Fall estimates.

587 ***Generalisation of the integrated bioenergetic and mass balance model***

588 Although there were a few discrepancies between eDNA and mark-recapture derived
589 estimates in abundance, these discrepancies still reflected a relatively high level of precision *across*

590 study populations, for which eDNA permitted broad differentiation across high- and low-
591 abundance populations. Although we advise caution, these results imply that eDNA can be used to
592 reliably estimate abundance and biomass in nature across populations. Furthermore, mark-
593 recapture estimates themselves can exhibit biases or fail when assumptions are violated. Our study
594 design does not allow us to identify which estimate (eDNA vs. Mark-recapture) is closer to the
595 'true' population size, and these issues would only be compounded in larger natural ecosystems.
596 Overall, we detected no systematic bias in eDNA-derived estimates related to lake size, mixing,
597 elevation, and population size. The integrated bioenergetics and mass balance approach that we
598 applied to the analysis of eDNA concentrations produced mostly accurate population abundance
599 estimates in small to medium-sized oligotrophic lakes. With further validation, such models have
600 the potential to be extended to other aquatic ecosystems.

601 Accounting for lake mixing was an important component of the mass-balance modelling
602 because the volume of the waterbody is a critical parameter in mass-balance modelling approaches.
603 Previous research has demonstrated that eDNA disperses throughout a lake and is roughly
604 homogenous during thermal mixing (Littlefair, Hrenchuk, et al., 2021). During lake stratification,
605 we found that the volume of the epilimnion is the appropriate volume input data, likely because
606 Brook Trout remains close to the surface during Summer (Tiberti et al., 2017). In contrast, when a
607 lake is undergoing thermal mixing, the volume of the entire lake is the appropriate volume input
608 data in the mass-balance model as eDNA is diluted across the entire lake, rather than just the
609 thermal layer inhabited by the target species (Littlefair, Hrenchuk, et al., 2021). We detected no
610 systematic bias related to lake thermal mixing and mixing explained no discrepancies between
611 eDNA and mark-recapture abundance estimates. The absence of overestimation of Brook Trout
612 abundance during mixing implies that the resuspension of sedimentary DNA during lake mixing

613 likely had a negligible impact on abundance estimates. This is despite lake sediments represent a
614 potentially potent source of eDNA (Turner et al., 2015). However, the amount of eDNA stored
615 within sediments and how it exchanges with the water column also depends on an organism's
616 spatial distribution, as well as biotic and abiotic conditions in water and at the water-sediment
617 interface (Capo et al., 2021). Sedimentary DNA re-suspension may be more important in other
618 types of lakes or for other species, particularly for systems inhabited by benthivorous fish species
619 that disturb sediment during feeding (e.g. Parkos et al., 2003).

620 ***Future directions: Can the nine lakes calibrate a model to predict abundance in novel systems?***

621 Our perspective on the future application of eDNA to estimate population abundance and
622 biomass is not to replace conventional methods, but rather to complement and/or improve upon
623 estimates generated by them. Notably, the integrated bioenergetic and mass-balance model
624 developed herein requires population size structure data which can only be obtained using mixed
625 mesh index gillnetting. These methods, often used in state and provincial monitoring programs to
626 estimate relative abundance based on CPUE (e.g. Zimmerman & Palo, 2011), require fewer
627 resources than mark-recapture techniques. To broadly apply eDNA to estimate abundance using
628 the methods and models developed herein also requires the establishment of a 'calibration system',
629 in which abundance estimated using conventional methods on a subset of ecosystems are used to
630 calibrate an eDNA/abundance model. Once calibrated, this model can be applied to estimate
631 abundance in other systems or time points lacking conventional estimates, by sampling eDNA and
632 the required physicochemical parameters.

633 However, our findings imply that the capacity to identify local predictors of k would be
634 particularly critical for such applications, as baseline data to estimate k rates within an individual
635 system substantially improved our model performance. To increase the reliability of abundance

636 estimates in freshwater systems derived from eDNA, further research is needed on eDNA dynamics
637 in lentic systems, with a particular focus on drivers of sedimentation and degradation rates. A
638 quantitative understanding of these interactions would allow us to better predict sedimentation and
639 degradation rates specific to local and temporal conditions. This would in turn likely improve the
640 integrated eDNA bioenergetic and mass-balance model performance as such dynamics could be
641 integrated into the modelling process. Additionally, such knowledge would facilitate the estimation
642 of the disappearance *k* parameter for lakes and time points outside of any putative "calibration
643 system" lakes simply by measuring the relevant environmental variables. Alternatively, a lake-side
644 small scale degradation experiment to estimate *k* could reduce the amount of mark-recapture data
645 needed to calibrate the model as the physiological parameters are more stable in space and time.

646 A growing number of individual studies on eDNA degradation have found that eDNA
647 degradation is the result of a complex combination of many variables such as pH, temperature, UV
648 radiation and microbial activity, and eDNA properties such as amplicon size and whether the
649 targeted gene is nuclear or mitochondrial (T. Jo et al., 2019; T. Jo & Minamoto, 2021; Saito & Doi,
650 2021b, 2021a; Strickler et al., 2015). Although temperature has emerged as a consistently impactful
651 parameter affecting eDNA degradation rates, the importance of other parameters such as UV,
652 microbial activity, eDNA source, and amplicon size remains to be confirmed (T. Jo & Minamoto,
653 2021; Lamb et al., 2022; Saito & Doi, 2021b). Collectively, we are still far from producing effective
654 eDNA degradation models, as few studies to date have examined the interaction between these
655 different environmental variables and eDNA properties (especially in natural ecosystems) and even
656 fewer have examined eDNA sedimentation. However, in the absence of controlled empirical
657 studies, further large-scale observational studies in natural ecosystems could facilitate the
658 identification of drivers of local eDNA decay rates. Experiments studying degradation dynamics

659 in natural ecosystems are thus crucial to facilitate and improve the adoption of eDNA to estimate
660 abundance in natural ecosystems.

661 Theoretical and empirical evidence suggests that eDNA production rate is related to fish
662 metabolic rate (Hervé et al., 2023; Thalinger et al., 2021; Yates et al., 2023; Yates, Glaser, et al.,
663 2021). However, to our knowledge, only one study to date has experimentally verified this
664 relationship under controlled empirical conditions and found a positive correlation between fish
665 activity rate, energy use, and eDNA shedding rate (Thalinger et al., 2021). The mass balance model
666 assumes eDNA production scales with body mass and is influenced by temperature-dependent
667 metabolic rates in poikilothermic Brook Trout (Hervé et al., 2023; Thalinger et al., 2021; Yates,
668 Cristescu, et al., 2021; Yates et al., 2023). We used a temperature-dependent metabolic function
669 (Hartman & Cox, 2008) to adjust for temperature effects on eDNA, though this may not fully reflect
670 eDNA production dynamics. While many studies have documented an effect of temperature on
671 eDNA production (e.g. Caza-Allard et al., 2022; T. Jo et al., 2019), whether this effect directly
672 reflects metabolic responses to temperature remains to be tested. Directly quantifying the eDNA
673 production temperature dependency function could thus improve model assumptions and
674 performance.

675 Our study additionally included mostly headwater lakes, so eDNA inputs from upstream
676 were considered equal to zero. However, this is rarely the case within a watershed. To add eDNA
677 transportation into the lake within the integrated model, data on both the inflow rate and the average
678 eDNA concentration in the inflow are required. In theory, these data can be implemented in
679 equation 4 (Chapra & Reckhow, 1983) such that:

680 $$[eDNA]_{Lake} \sim \frac{I_0 \sum_{i=1}^{N} (M_i^b) \times f(T) + Q_{in}[inflow]}{Q_{out} + kV} \quad (9)$$

Where Q_{in} is the inflow rate, Q_{out} is the outflow rate, and $[inflow]$ is the mean eDNA concentration of the inflow.

Conclusion

Our study proposes an integrated bioenergetics and mass-balance approach to relate eDNA concentration to population abundance estimation. Our integrated eDNA model performed well at estimating abundance, and it facilitated total abundance and biomass estimates that were comparable to conventional mark-recapture methodologies, often considered a 'gold-standard' for population abundance estimates. We show that eDNA can detect both spatial and temporal differences in fish abundance, provided the equilibrium assumptions of the model are respected. To respect these assumptions, we recommend avoiding sampling ten to twenty days after known fluctuations in abundance (e.g. harvest), depending on the eDNA degradation rate and outflow flux. Overall, the results of this study represent an important advancement in the use of eDNA to quantify total population abundance, with strong implications for the application of eDNA for abundance estimates in a context of ecosystem management. The quantitative analysis of eDNA, applied with an integrated bioenergetics and mass-balance approach, could provide a cost-effective, precise, and accurate tool for managers and researchers. This is critical in an era where the acquisition of population abundance data is increasingly important for biodiversity management (e.g. Canals et al., 2021; Fonseca et al., 2023; Kelly et al., 2024).

References

Albert, J. S., Destouni, G., Duke-Sylvester, S. M., Magurran, A. E., Oberdorff, T., Reis, R. E., Winemiller, K. O., & Ripple, W. J. (2021). Scientists' warning to humanity on the freshwater biodiversity crisis. *Ambio*, *50*(1), 85–94. https://doi.org/10.1007/s13280-020-01318-8

Allegier, J. E., Wenger, S. J., Rosemond, A. D., Schindler, D. E., & Layman, C. A. (2015). Metabolic theory and taxonomic identity predict nutrient recycling in a diverse food web. *PNAS*, *112 (20)*. https://doi.org/10.1073/pnas.1420819112

Beaulieu, J., Gheta, M., & Macdonald, A. A. M. (2024). *Using Taylor Expansions to fit power law functions*. https://julien-beaulieu.github.io/taylor-expansions-stats.github.io/vignette_taylor_series.html

Bonar, S. A., Hubert, W. A., & Willis, D. W. (2009). *Standard methods for sampling North American freshwater fishes*. American Fisheries Society.

Brandão-Dias, P. F. P., Hallack, D. M. C., Snyder, E. D., Tank, J. L., Bolster, D., Volponi, S., Shogren, A. J., Lamberti, G. A., Bibby, K., & Egan, S. P. (2023). Particle size influences decay rates of environmental DNA in aquatic systems. *Molecular Ecology Resources*, *23*(4), 756–770. https://doi.org/10.1111/1755-0998.13751

Bürkner, P. C. (2018). Advanced Bayesian multilevel modeling with the R package brms. *R Journal*, *10*(1), 395–411. https://doi.org/10.32614/rj-2018-017

Buuren, S. van, & Groothuis-Oudshoorn, K. (2011). mice : Multivariate Imputation by Chained Equations in R. *Journal of Statistical Software*, *45*(3), 1–67. https://doi.org/10.18637/jss.v045.i03

Canals, O., Mendibil, I., Santos, M., Irigoien, X., & Rodríguez-Ezpeleta, N. (2021). Vertical stratification of environmental DNA in the open ocean captures ecological patterns and behavior of deep-sea fishes. *Limnology And Oceanography Letters*, *6*(6), 339–347. https://doi.org/10.1002/lol2.10213

Capo, E., Giguet-Covex, C., Rouillard, A., Nota, K., Heintzman, P. D., Vuillemin, A., Ariztegui, D., Arnaud, F., Belle, S., Bertilsson, S., Bigler, C., Bindler, R., Brown, A. G., Clarke, C. L., Crump, S. E., Debroas, D., Englund, G., Ficetola, G. F., Garner, R. E., … Parducci, L. (2021). Lake Sedimentary DNA Research on Past Terrestrial and Aquatic Biodiversity: Overview and Recommendations. *Quaternary*, *4*(1), 6. https://doi.org/10.3390/quat4010006

Carraro, L., Hartikainen, H., Jokela, J., Bertuzzo, E., & Rinaldo, A. (2018). Estimating species distribution and abundance in river networks using environmental DNA. *Proceedings of the National Academy of Sciences*, *115*(46), 11724–11729. https://doi.org/10.1073/pnas.1813843115

Caza-Allard, I., Laporte, M., Côté, G., April, J., & Bernatchez, L. (2022). Effect of biotic and abiotic factors on the production and degradation of fish environmental DNA: An experimental evaluation. *Environmental DNA*, *4*(2), 453–468. https://doi.org/10.1002/edn3.266

Chapra, S. C., & Reckhow, K. H. (1983). *Ingeneering Approaches for Lake Management. Volume 2: Mechanistic Modeling*. Butterworth.

CoreTeam, R. (2020). *R: A language and environment for statistical computing*. R Foundation for Statistical Computing. https://www.r-project.org

Deslauriers, D., Chimpps, S. R., Breck, J. E., Rice, J. A., & Madenjian, C. P. (2017). Fiash Bioenergetic 4.0: An R-based Modeling Application. *Fisheries*, *42*(11), 586–596.

Dunker, K. J., Sepulveda, A. J., Massengill, R. L., Olsen, J. B., Russ, O. L., Wenburg, J. K., & Antonovich, A. (2016). Potential of environmental DNA to evaluate northern pike (Esox lucius) eradication efforts: An experimental test and case study. *PLoS ONE*, *11*(9), 1–21. https://doi.org/10.1371/journal.pone.0162277

Environment and Natural Ressources Canada. (2024). *Real-Time Hydrometric Data*. https://wateroffice.ec.gc.ca/map/index_e.html

Ficetola, G. F., Miaud, C., Pompanon, F., & Taberlet, P. (2008). Species detection using environmental DNA from water samples. *Biology Letters*, *4*(4), 423–425. https://doi.org/10.1098/rsbl.2008.0118

Fonseca, V. G., Davison, P. I., Creach, V., Stone, D., Bass, D., & Tidbury, H. J. (2023). The Application of eDNA for Monitoring Aquatic Non-Indigenous Species: Practical and Policy Considerations. *Diversity*, *15*(5), 1–17. https://doi.org/10.3390/d15050631

Gaudet-Boulay, M., García-Machado, E., Laporte, M., Yates, M., Bougas, B., Hernandez, C., Côté, G., Gilbert, A., & Bernatchez, L. (2023). Relationship between brook charr (Salvelinus fontinalis) eDNA concentration and angling data in structured wildlife areas. *Environmental DNA*, *5*(5), 861–879. https://doi.org/10.1002/edn3.341

Hanson, P. C., Johnson, T. B., Schindler, D. E., & Kitchell, J. F. (1997). Fish Bioenergetics 3.0. *World Wide Web Internet And Web Information Systems*.

Hartman, K. J., & Cox, M. K. (2008). Refinement and Testing of a Brook Trout Bioenergetics Model. *Transactions of the American Fisheries Society*, *137*(1), 357–363. https://doi.org/10.1577/t05-243.1

Hervé, A., Domaizon, I., Baudoin, J. M., Dejean, T., Gibert, P., Valentini, A., & Logez, M. (2023). Do temperature and population size structure influence the quantity of fish eDNA in water? *Frontiers in Environmental Science*, *11*(July), 1–6. https://doi.org/10.3389/fenvs.2023.1193393

Ho, L. T., & Goethals, P. L. M. (2019). Opportunities and Challenges for the Sustainability of Lakes and Reservoirs in Relation to the Sustainable Development Goals (SDGs). *Water*, *11*(7), 1462. https://doi.org/10.3390/w11071462

Howarth, A., Nguyen, V. M., & Cooke, S. J. (2023). Managing Canadian freshwater fisheries: persistent challenges and emerging opportunities. *Canadian Journal of Fisheries and Aquatic Sciences*, *80*(9), 1436–1455. https://doi.org/10.1139/cjfas-2023-0011

Huang, S., Yoshitake, K., Watabe, S., & Asakawa, S. (2022). Environmental DNA study on aquatic ecosystem monitoring and management: Recent advances and prospects. *Journal of Environmental Management*, *323*(March), 116310. https://doi.org/10.1016/j.jenvman.2022.116310

Hubert, W. A., Pope, K. L., & Dettmers, J. M. (2012). Passive capture techniques. In *A. V. Zale, D. L. Parrish, & T. . Sutton (Eds.), Fisheries Techniques* (3rd ed.). American Fisheries Society.

Jane, S. F., Wilcox, T. M., Mckelvey, K. S., Young, M. K., Schwartz, M. K., Lowe, W. H., Letcher, B. H., & Whiteley, A. R. (2015). Distance, flow and PCR inhibition: EDNA dynamics in two

headwater streams. *Molecular Ecology Resources*, *15*(1), 216–227. https://doi.org/10.1111/1755-0998.12285

Jerde, C. L. (2019). Can we manage fisheries with the inherent uncertainty from eDNA? *Journal of Fish Biology*, *98*, 341353. https://doi.org/10.1111/jfb.14218

Jo, T., & Minamoto, T. (2021). Complex interactions between environmental DNA (eDNA) state and water chemistries on eDNA persistence suggested by meta-analyses. *Molecular Ecology Resources*, *21*(5), 1490–1503. https://doi.org/10.1111/1755-0998.13354

Jo, T., Murakami, H., Yamamoto, S., Masuda, R., & Minamoto, T. (2019). Effect of water temperature and fish biomass on environmental DNA shedding, degradation, and size distribution. *Ecology and Evolution*, *9*(3), 1135–1146. https://doi.org/10.1002/ece3.4802

Jo, T. S. (2023). Correlation between the number of eDNA particles and species abundance is strengthened by warm temperature: simulation and meta-analysis. *Hydrobiologia*, *850*(1), 39–50. https://doi.org/10.1007/s10750-022-05036-y

Johnson, L. (1983). Homeostatic Characteristics of Single Species Fish Stocks in Arctic Lakes. *Canadian Journal of Fisheries and Aquatic Sciences*, *40*(7), 987–1024. https://doi.org/10.1139/f83-125

Kagzi, K., Hechler, R. M., Fussmann, G. F., & Cristescu, M. E. (2022). Environmental RNA degrades more rapidly than environmental DNA across a broad range of pH conditions. *Molecular Ecology Resources*, *22*(7), 2640–2650. https://doi.org/10.1111/1755-0998.13655

Kelly, R. P., Lodge, D. M., Lee, K. N., Theroux, S., Sepulveda, A. J., Scholin, C. A., Craine, J. M., Andruszkiewicz Allan, E., Nichols, K. M., Parsons, K. M., Goodwin, K. D., Gold, Z., Chavez, F. P., Noble, R. T., Abbott, C. L., Baerwald, M. R., Naaum, A. M., Thielen, P. M., Simons,

A. L., … Weisberg, S. B. (2024). Toward a national eDNA strategy for the United States. *Environmental DNA*, *6*(1), 1–10. https://doi.org/10.1002/edn3.432

Krebs, C. J. (2009). Estimating Abundance in Animal and Plant Populations. In *Ecology: The experimental analysis of distribution and abundance* (6th ed.). Pearson Benjamin Cummings.

Lamb, P. D., Fonseca, V. G., Maxwell, D. L., & Nnanatu, C. C. (2022). Systematic review and meta-analysis: Water type and temperature affect environmental DNA decay. *Molecular Ecology Resources*, *22*(7), 2494–2505. https://doi.org/10.1111/1755-0998.13627

Littlefair, J. E., Hrenchuk, L. E., Blanchfield, P. J., Rennie, M. D., & Cristescu, M. E. (2021). Thermal stratification and fish thermal preference explain vertical eDNA distributions in lakes. *Molecular Ecology*, *30*(13), 3083–3096. https://doi.org/10.1111/mec.15623

Littlefair, J. E., Rennie, M. D., & Cristescu, M. E. (2021). Environmental nucleic acids: a field-based comparison for monitoring freshwater habitats using eDNA and eRNA. *BioRxiv*, 2021.12.01.469845. https://www.biorxiv.org/content/10.1101/2021.12.01.469845v1%0Ahttps://www.biorxiv.org/content/10.1101/2021.12.01.469845v1.abstract

Matte, J. M. O., Glaser, D. M., Post, J. R., & Fraser, D. J. (2023). Contrasting demographic responses to size-selective harvesting among neighbouring wild fish populations. *Journal of Applied Ecology*, *April*. https://doi.org/10.1111/1365-2664.14420

McElreath, R. (2018). *Statistical rethinking: A Bayesian course with examples in R and Stan* (Chapman an).

Messner, J. S., Maclennan, M. M., & Vinebrooke, R. D. (2013). Higher temperatures enhance the effects of invasive sportfish on mountain zooplankton communities. *Freshwater Biology*, *58*(2), 354–364. https://doi.org/10.1111/fwb.12062

Morgan, G. E. (2002). *Manual of instructions - fall walleye index netting (FWIN)*.

Ogle, D. H. (2015). *Introductory Fisheries Analyses with R*. Chapman & Hall.

Parkos, J. J., Santucci, V. J., & Wahl, D. H. (2003). Effects of adult common carp (Cyprinus carpio) on multiple trophic levels in shallow mesocosms. *Canadian Journal of Fisheries and Aquatic Sciences*, *60*(2), 182–192. https://doi.org/10.1139/f03-011

Parsley, M. B., Crespi, E. J., Rittenhouse, T. A. G., Brunner, J. L., & Goldberg, C. S. (2024). Environmental DNA concentrations vary greatly across productive and degradative conditions, with implications for the precision of population estimates. *Scientific Reports*, *14*(1), 17392. https://doi.org/10.1038/s41598-024-66732-4

Pont, D. (2024). Predicting downstream transport distance of fish eDNA in lotic environments. *Molecular Ecology Resources*, *24*(4), 1–14. https://doi.org/10.1111/1755-0998.13934

Post, J. R., Parkinson, E. A., & Johnston, N. T. (1999). Density-dependent processes in structured fish populations: Interaction strengths in whole-lake experiments. *Ecological Monographs*, *69*(2), 155–175. https://doi.org/10.1890/0012-9615(1999)069[0155:DDPISF]2.0.CO;2

Post, J. R., Sullivan, M., Cox, S., Lester, N. P., Walters, C. J., Parkinson, E. A., Paul, A. J., Jackson, L., & Shuter, B. J. (2002). Canada's Recreational Fisheries: The Invisible Collapse? *Fisheries*, *27*(1), 6–17. https://doi.org/10.1577/1548-8446(2002)027<0006:crf>2.0.co;2

Rourke, M. L., Fowler, A. M., Hughes, J. M., Broadhurst, M. K., DiBattista, J. D., Fielder, S., Wilkes Walburn, J., & Furlan, E. M. (2022). Environmental DNA (eDNA) as a tool for assessing fish biomass: A review of approaches and future considerations for resource surveys. *Environmental DNA*, *4*(1), 9–33. https://doi.org/10.1002/edn3.185

Saito, T., & Doi, H. (2021a). A Model and Simulation of the Influence of Temperature and Amplicon Length on Environmental DNA Degradation Rates: A Meta-Analysis Approach. *Frontiers in Ecology and Evolution*, *9*(March), 1–8. https://doi.org/10.3389/fevo.2021.623831

Saito, T., & Doi, H. (2021b). *Degradation modeling of water environmental DNA : Experiments on multiple DNA sources in pond and seawater*. *August 2020*, 850–860. https://doi.org/10.1002/edn3.192

Sassoubre, L. M., Yamahara, K. M., Gardner, L. D., Block, B. A., & Boehm, A. B. (2016). Quantification of Environmental DNA (eDNA) Shedding and Decay Rates for Three Marine Fish. *Environmental Science and Technology*, *50*(19), 10456–10464. https://doi.org/10.1021/acs.est.6b03114

Schnabel, Z. E. (1938). The Estimation of the Total Fish Population of a Lake. *The American Mathematical Monthly*, *45*(6), 348–352. https://doi.org/10.1080/00029890.1938.11990818

Seber, G. A. F. (2002). *The Estimation of Animal Abundance and Related Parameters* (B. Publishing, Ed.; 2 nd).

Sepulveda, A. J., Nelson, N. M., Jerde, C. L., & Luikart, G. (2020). Are Environmental DNA Methods Ready for Aquatic Invasive Species Management? *Trends in Ecology & Evolution*, *35*(8), 668–678. https://doi.org/10.1016/j.tree.2020.03.011

Shogren, A. J., Tank, J. L., Andruszkiewicz, E., Olds, B., Mahon, A. R., Jerde, C. L., & Bolster, D. (2017). Controls on eDNA movement in streams: Transport, Retention, and Resuspension. *Scientific Reports*, *7*(1), 5065. https://doi.org/10.1038/s41598-017-05223-1

Stewart, K. A. (2019). Understanding the effects of biotic and abiotic factors on sources of aquatic environmental DNA. *Biodiversity and Conservation*, *28*, 983–1001. https://doi.org/10.1007/s10531-019-01709-8

Strickler, K. M., Fremier, A. K., & Goldberg, C. S. (2015). Quantifying effects of UV-B, temperature, and pH on eDNA degradation in aquatic microcosms. *Biological Conservation*, *183*, 85–92. https://doi.org/10.1016/j.biocon.2014.11.038

Thalinger, B., Rieder, A., Teuffenbach, A., Pütz, Y., Schwerte, T., Wanzenböck, J., & Traugott, M. (2021). The Effect of Activity, Energy Use, and Species Identity on Environmental DNA Shedding of Freshwater Fish. *Frontiers in Ecology and Evolution*, *9*(February), 1–13. https://doi.org/10.3389/fevo.2021.623718

Thornton, K. W., & Lessem, A. S. (1978). A Temperature Algorithm for Modifying Biological Rates. *Transactions of the American Fisheries Society*, *107*, 284–287. https://doi.org/10.1577/1548-8659(1978)107<284

Tiberti, R., Nelli, L., Brighenti, S., Iacobuzio, R., & Rolla, M. (2017). Spatial distribution of introduced brook trout Salvelinus fontinalis (Salmonidae) within alpine lakes: Evidences from a fish eradication campaign. *European Zoological Journal*, *84*(1), 73–88. https://doi.org/10.1080/11250003.2016.1274436

Trépanier-Leroux, D., Yates, M. C., Astorg, L., Fraser, D. J., Humphries, S., Cristescu, M. E., & Derry, A. M. (2023). Density-dependent effects of exotic brook trout on aquatic communities

in mountain lakes revealed by environmental DNA and morphological taxonomy. *Hydrobiologia*, *851*, 1489–1512. https://doi.org/10.1007/s10750-023-05398-x

Turner, C. R., Uy, K. L., & Everhart, R. C. (2015). Fish environmental DNA is more concentrated in aquatic sediments than surface water. *Biological Conservation*, *183*, 93–102. https://doi.org/10.1016/j.biocon.2014.11.017

Vanni, M. J., & McIntyre, P. B. (2016). Predicting nutrient excretion of aquatic animals with metabolic ecology and ecological stoichiometry: A global synthesis. *Ecology*, *97*(12), 3460–3471. https://doi.org/10.1002/ecy.1582

Ward, H. G. M., Askey, P. J., Post, J. R., Varkey, D. A., & McAllister, M. K. (2012). Basin characteristics and temperature improve abundance estimates from standard index netting of rainbow trout (Oncorhynchus mykiss) in small lakes. *Fisheries Research*, *131–133*, 52–59. https://doi.org/10.1016/j.fishres.2012.07.011

Wilcox, T. M., McKelvey, K. S., Young, M. K., Jane, S. F., Lowe, W. H., Whiteley, A. R., & Schwartz, M. K. (2013). Robust detection of rare species using environmental DNA: the importance of primer specificity. *PloS One*, *8*(3), e59520. https://doi.org/10.1371/journal.pone.0059520

Yates, M. C., Cristescu, M. E., & Derry, A. M. (2021). Integrating physiology and environmental dynamics to operationalize environmental DNA (eDNA) as a means to monitor freshwater macro-organism abundance. *Molecular Ecology*, *March*, 1–20. https://doi.org/10.1111/mec.16202

Yates, M. C., Fraser, D. J., & Derry, A. M. (2019). Meta-analysis supports further refinement of eDNA for monitoring aquatic species-specific abundance in nature. *Environmental DNA*, *1*(1), 5–13. https://doi.org/10.1002/edn3.7

Yates, M. C., Glaser, D. M., Post, J. R., Cristescu, M. E., Fraser, D. J., & Derry, A. M. (2021). The relationship between eDNA particle concentration and organism abundance in nature is strengthened by allometric scaling. *Molecular Ecology*, *30*(13), 3068–3082. https://doi.org/10.1111/mec.15543

Yates, M. C., Wilcox, T. M., McKelvey, K. S., Young, M. K., Schwartz, M. K., & Derry, A. M. (2021). Allometric scaling of eDNA production in stream-dwelling brook trout (Salvelinus fontinalis) inferred from population size structure. *Environmental DNA*, *3*(3), 553–560. https://doi.org/10.1002/edn3.150

Yates, M. C., Wilcox, T. M., Stoeckle, M. Y., & Heath, D. D. (2023). Interspecific allometric scaling in eDNA production among northwestern Atlantic bony fishes reflects physiological allometric scaling. *Environmental DNA*, *5*(5), 1105–1115. https://doi.org/10.1002/edn3.381

Zimmerman, J. K. M., & Palo, R. T. (2011). Reliability of catch per unit effort (CPUE) for evaluation of reintroduction programs – A comparison of the mark-recapture method with standardized trapping. *Knowledge and Management of Aquatic Ecosystems*, *401*, 07. https://doi.org/10.1051/kmae/2011016

Table 1. Parameter estimates and Bayes R^2 for the linear regression, allometrically scaled biomass regression and the mass balance model. The formula column refers to the formula of the model specified as equations in the method section. The numbers in parentheses represent the 95 % credible interval on parameter estimates. The Bayes R^2 reported are the mean of the Bayes R^2 of each model iteration. b is the allometric coefficient, k is the sum of the degradation and sedimentation constant, I_0 is the eDNA generation coefficient, β is the slope of the linear model, sigma is the variance. The coefficient $\beta_{ln(k)\ Temperature}$ is the regression coefficient of the effect of water temperature on k. Sd stands for standard deviation.

Model	Bayes R^2	looIC	b	$ln(k)$	Sd(ln(k))	$\beta_{ln(k)\ Temperature}$	Ln(I_0) or β	Sd(ln(I_0))	Sigma	Formula
Linear regression	0.24	650.4	-	-	-	-	0.13 (0.05-0.21)	-	2387 (1889-3037)	equation 6
Allometrically scaled biomass	0.44	645.0	0.58 (0.25-0.89)	-	-	-	0.03 (-1.4-1.43)	-	2162.93 (1707-2775)	equation 7
Mass balance eDNA	0.71	640.5	0.67 (0.28-0.98)	-0.70 (-0.90-0.51)	0.29 (0.02-0.70)	0.1 (0.02-0.18)	10.52 (8.94-12.31)	-	θ = 5.13 (4.46-5.88) α = 0.13 (0.06-0.17)	equation 5
Mass balance with N as dependent variable, with lake specific and temperature dependant k and sampling period specific I_0	0.75	550.8	0.79 (0.45-0.98)	-0.76 (-1.74-0.21)	0.30 (0.06-0.65)	0.12 (0.06-0.18)	10.36 (8.85-12.11)	0.19 (0.01-0.60)	θ = 1.94 (0.52-3.35) α = 0.18 (0.13-0.22)	equation 8
Mass balance with N as dependent variable without sampling period specific I_0	0.75	547.0	0.8 (0.49-0.98)	-0.7 (-0.9--0.51)	0.3 (0.06-0.66)	0.13 (0.07-0.19)	10.46 (9.28-12.01)	-	θ = 2.14 (0.83-3.47) α = 0.18 (0.12-0.22)	equation 8.1
Mass balance with N as dependent variable without lake specific k nor sampling period specific I_0	0.51	563.6	0.47 (0.06-0.96)	0.49 (0.4-0.59)	-	-	10.60 (8.23-12.47)	-	θ = 2.75 (1.55-3.98) α = 0.17 (0.11-0.21)	equation 8.2

Table 2. Parameter estimates for bias testing. The Bayes R^2 reported is the mean of the Bayes R^2 of each draw. The dependent variable is the z-score of each total Brook Trout population abundance estimate, calculated as the estimate from eDNA minus the estimate from mark-recapture divided by the standard deviation of the draws of the estimate from eDNA. CI stands for credible interval.

Variable	Parameter estimate	CI (95 %)	Bayes R^2
Total abundance	-0.00018	-0.0017 – 0.0013	0.33
Lake area	-0.026	-0.22 – 0.22	
Mixing (yes)	0.075	-1.89 – 2.03	
Elevation	-0.00043	-0.0032 – 0.0024	
Season (Fall)	-0.35	-2.27 – 1.57	
Treatment (Harvest)	0.3	-1.16 – 1.76	
Elevation*Mixing	-0.0008	-0.0023 – 0.0008	
Elevation*Season	0.0007	-0.0008 – 0.0024	
Season*Treatment	0.87	-0.77 – 2.51	

List of figures

Figure 1. Map of the study area showing the locations of the lakes included in the research.

Figure 2. Comparison of model performance relating eDNA concentration to total population abundance. The black line represents the 1:1 slope, while the red line shows the linear regression between the predicted and measured eDNA concentrations. Parameter estimates and R^2 values for each model are provided in Table 2.

Figure 3. Total population abundance estimates from eDNA for all the populations and sampling periods. The thick colored line represents the 50 % credible interval of eDNA estimates, while the thin colored lines represent the 95 % credible intervals. Grey lines and dots represent the 95% credible interval and mean from the mark-recapture abundance estimates. eDNA estimates are derived from the full mass balance model (Equation 8).

Figure 4. Total population abundance estimates from the eDNA mass balance model (red) and mark-recapture (blue). eDNA estimates are produced from the fitted mass balance model with sampling period specific eDNA generation coefficient (I_0) (Equation 8). Lakes that were harvested are marked with an asterisk (*).

Figure 5. Population biomass estimated from the eDNA mass balance model and mark-recapture. In a) the x axis is the biomass estimated from the mark-recapture abundance estimates and the y axis is the biomass estimated from the eDNA mass balance model. The red line is the linear regression between the two, and the black line is the 1:1 slope. In b) to j) the biomass estimated from the eDNA mass balance model (red) and the biomass estimated from the mark-recapture (blue). eDNA estimates are produced from the fitted mass balance model with sampling period specific eDNA generation coefficient (I0) (equation 8.2). Lakes that were harvested are marked with an asterisk (*).

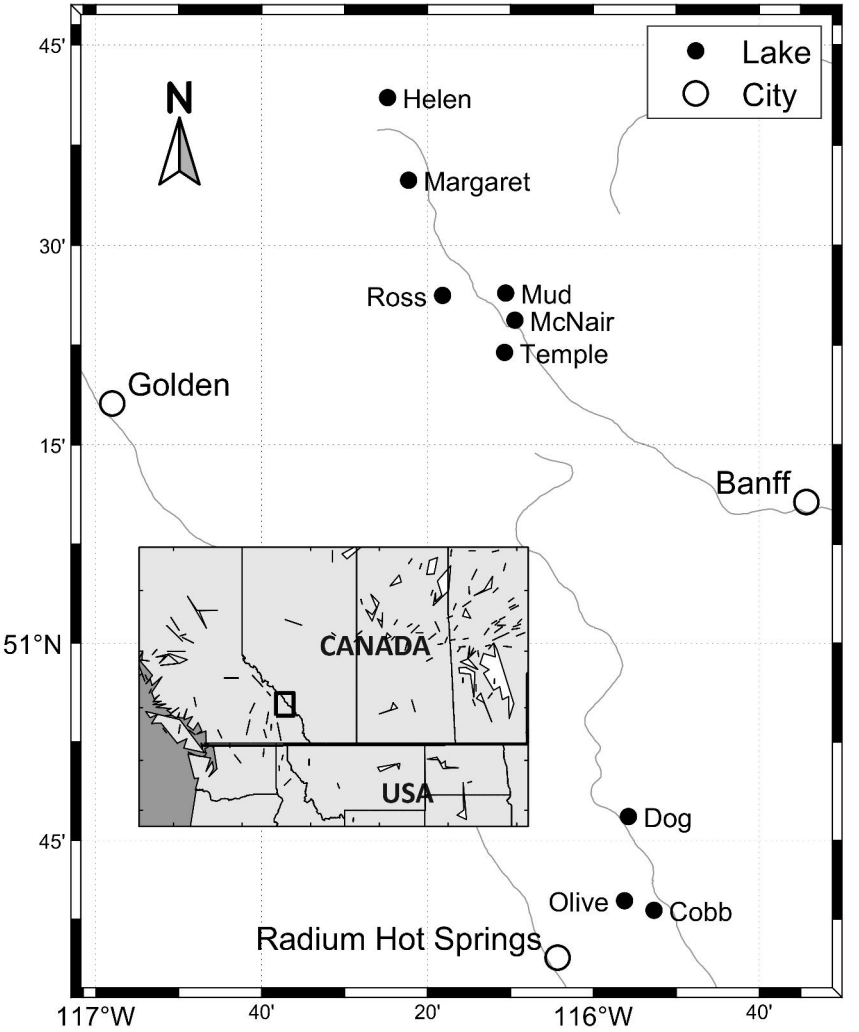
Lake
City
N
Helen
Margaret
Ross
Mud
McNair
Temple
Golden
Banff
CANADA
USA
Dog
Olive
Cobb
Radium Hot Springs
45'
30'
15'
51°N
45'
117°W
40'
20'
116°W
40'

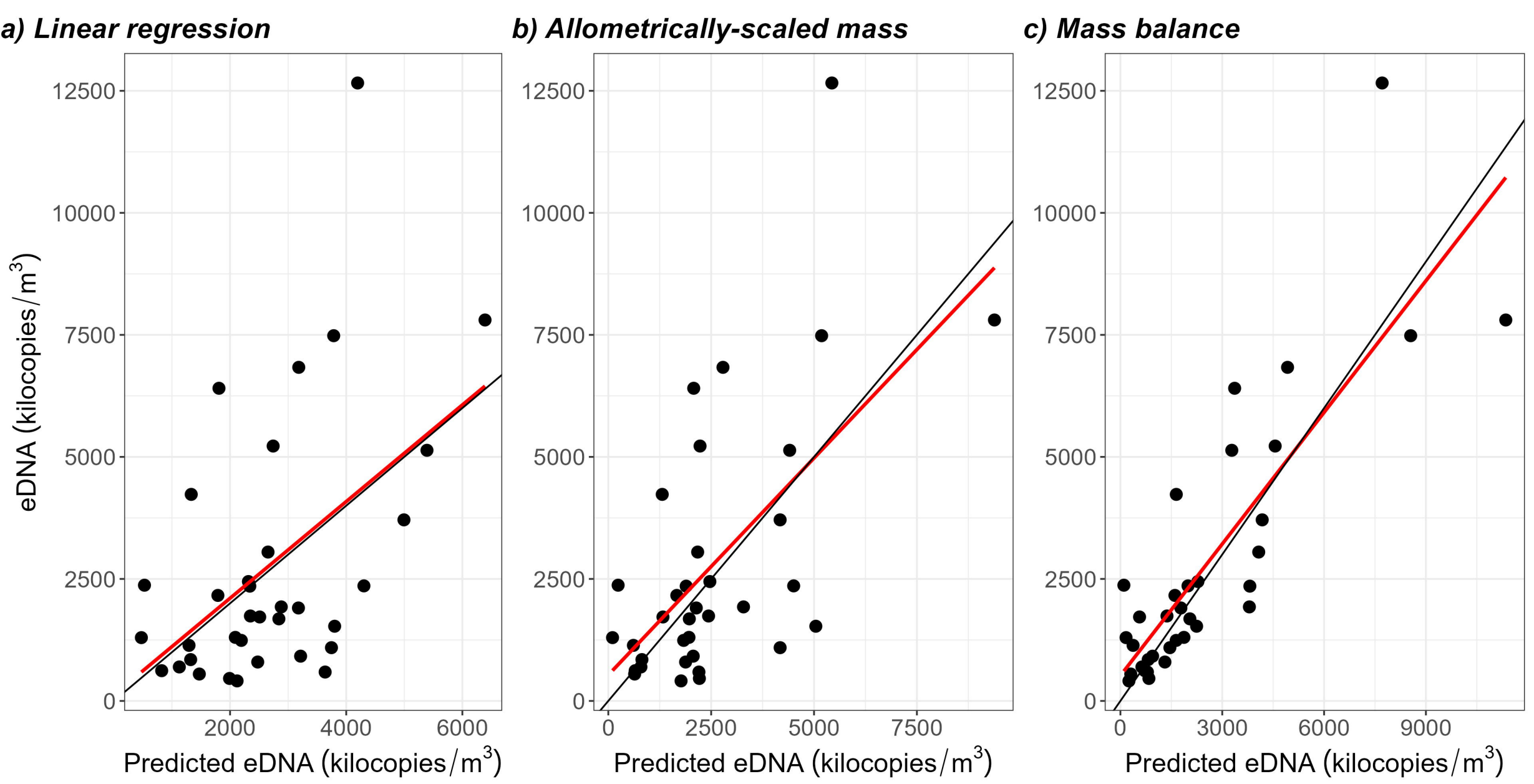
a) Linear regression
b) Allometrically-scaled mass
c) Mass balance
eDNA (kilocopies/m3)
Predicted eDNA (kilocopies/m3)
0
2500
5000
7500
10000
12500
2000
4000
6000
0
2500
5000
7500
0
3000
6000
9000

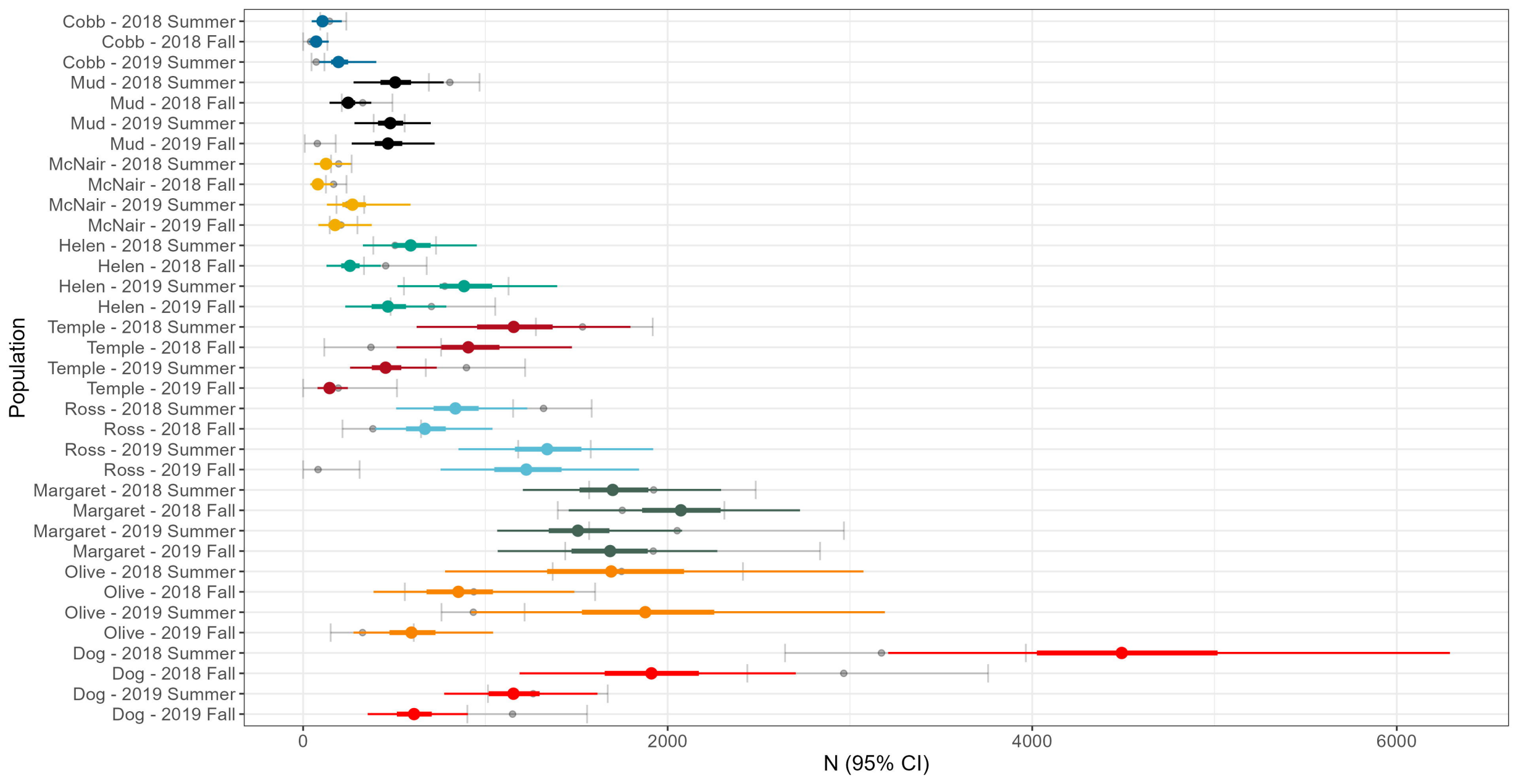
Population
Cobb - 2018 Summer
Cobb - 2018 Fall
Cobb - 2019 Summer
Mud - 2018 Summer
Mud - 2018 Fall
Mud - 2019 Summer
Mud - 2019 Fall
McNair - 2018 Summer
McNair - 2018 Fall
McNair - 2019 Summer
McNair - 2019 Fall
Helen - 2018 Summer
Helen - 2018 Fall
Helen - 2019 Summer
Helen - 2019 Fall
Temple - 2018 Summer
Temple - 2018 Fall
Temple - 2019 Summer
Temple - 2019 Fall
Ross - 2018 Summer
Ross - 2018 Fall
Ross - 2019 Summer
Ross - 2019 Fall
Margaret - 2018 Summer
Margaret - 2018 Fall
Margaret - 2019 Summer
Margaret - 2019 Fall
Olive - 2018 Summer
Olive - 2018 Fall
Olive - 2019 Summer
Olive - 2019 Fall
Dog - 2018 Summer
Dog - 2018 Fall
Dog - 2019 Summer
Dog - 2019 Fall
0
2000
4000
6000
N (95% CI)

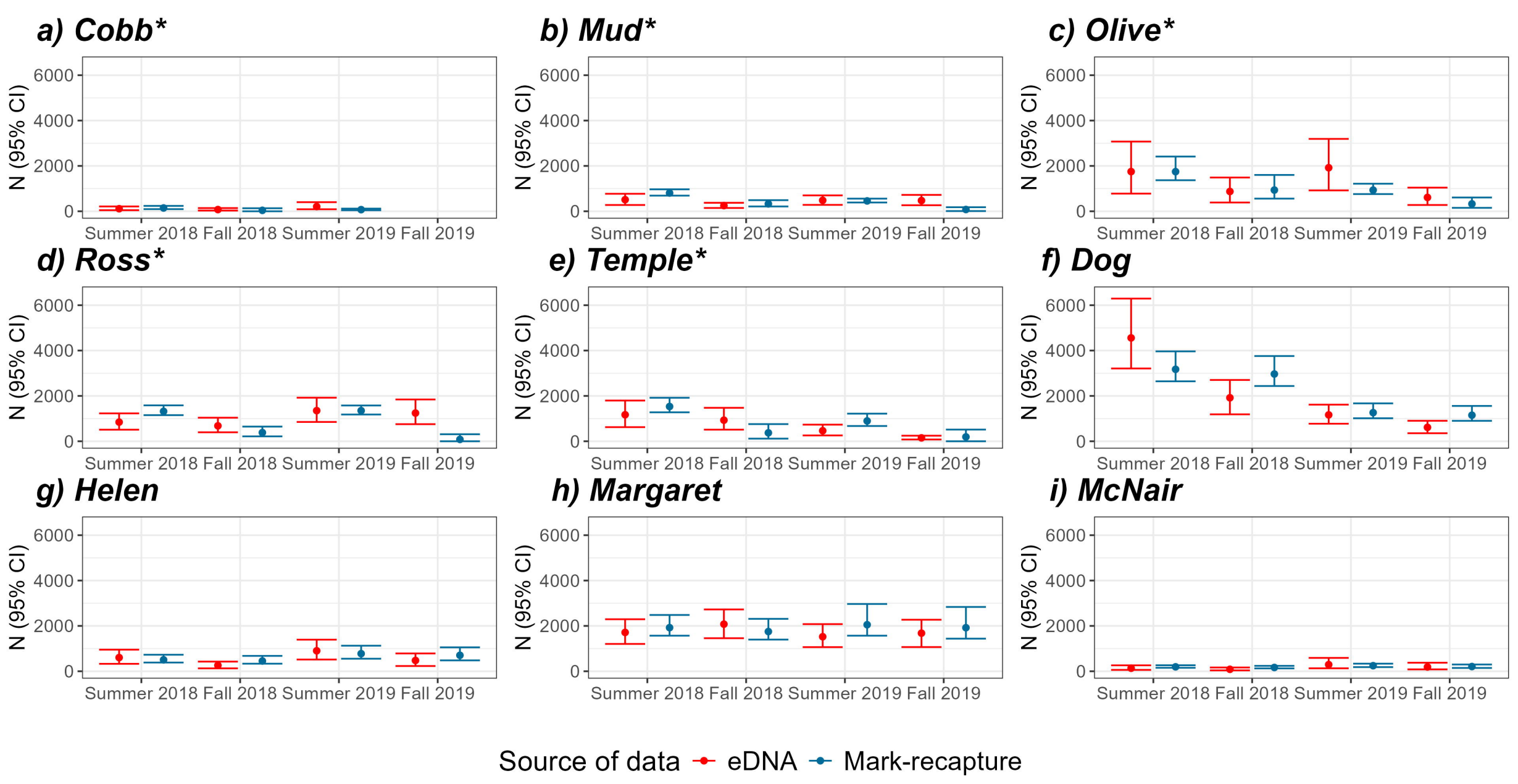
a) Cobb*
b) Mud*
c) Olive*
d) Ross*
e) Temple*
f) Dog
g) Helen
h) Margaret
i) McNair
N (95% CI)
0
2000
4000
6000
Summer 2018
Fall 2018
Summer 2019
Fall 2019
Source of data
eDNA
Mark-recapture

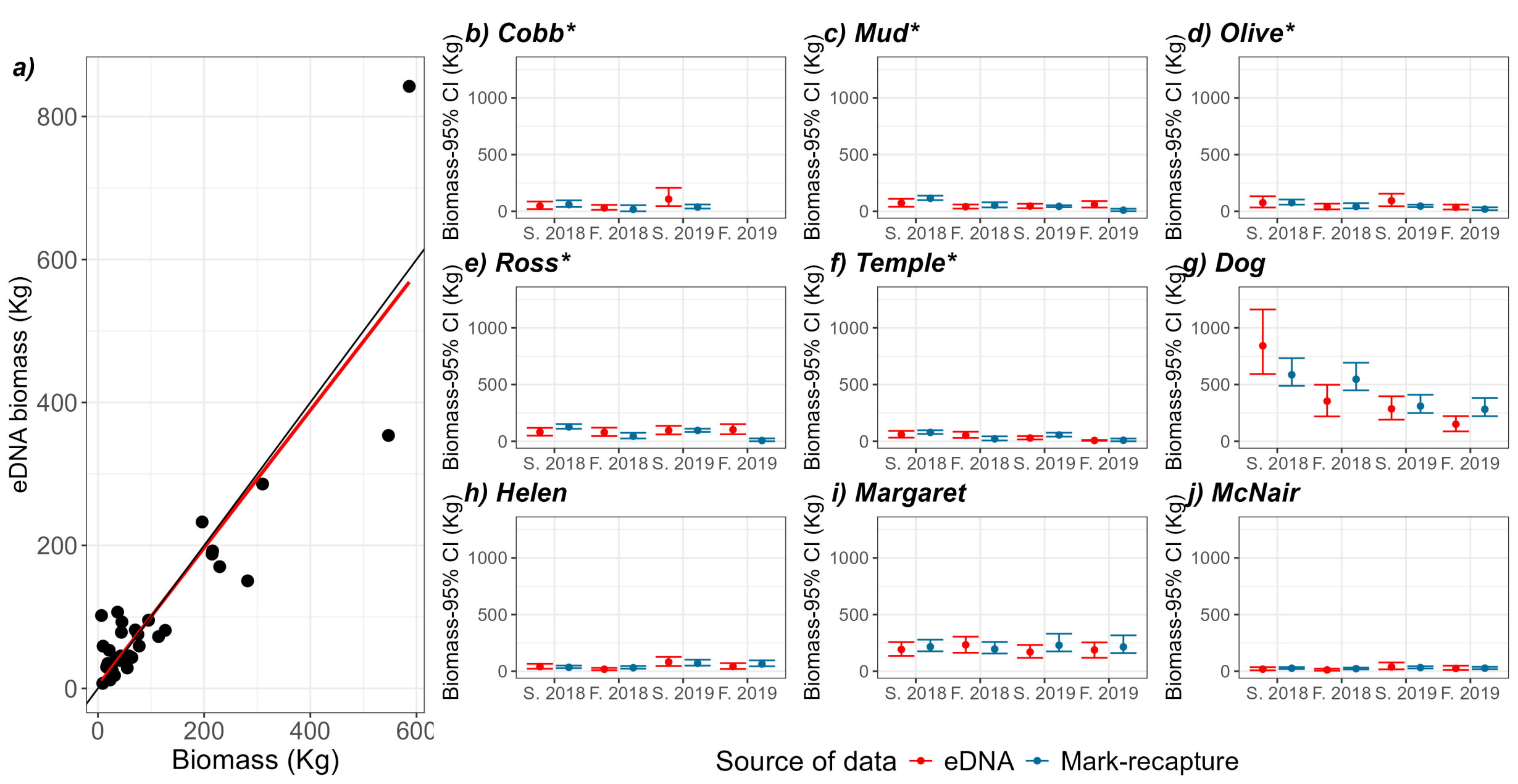
a)
eDNA biomass (Kg)
Biomass (Kg)
0
200
400
600
800
b) Cobb*
c) Mud*
d) Olive*
e) Ross*
f) Temple*
g) Dog
h) Helen
i) Margaret
j) McNair
Biomass-95% CI (Kg)
1000
500
S. 2018
F. 2018
S. 2019
F. 2019
Source of data
eDNA
Mark-recapture